Nanovesicles derived from protocorm-like bodies ofDendrobium officinal enhance corneal epithelial repair and reduce inflammation in dry eye disease models

Recommended Citation

Nanovesicles derived from protocorm-like bodies of Dendrobium officinal enhance corneal epithelial repair and reduce inflammation in dry eye disease models

Bao Yuqing [a,b,d], Peng Chengyu [a,b,c,d], Zhang Fenglei [c,d,e], Zheng Yuqiang [c,d,e], Zhang Mingqi [c,d,e,**,1], He Wei [a,b,c,d,e,*,1]

[a] Jinzhou Medical University, China
[b] He Eye Specialist Hospital, China
[c] Stem Cell Center of Precision Medicine Innovation Institute, He University, China
[d] Liaoning Key Lab of Ophthalmic Stem Cells, He University, China
[e] School of Pharmacy, He University, China

Abstract

Plant-derived nanovesicles (PDNVs) offer a promising, biocompatible therapeutic platform. In this study, we isolated nanovesicles from protocorm-like bodies of Dendrobium officinale (PLBs-NVs) and evaluated their efficacy in dry eye disease (DED) models. PLBs-NVs protected human corneal epithelial cells against hyperosmotic stress, supported wound repair, and inhibited inflammation *in vitro*. In a desiccating stress-induced DED mouse model, topical PLBs-NVs treatment significantly restored tear secretion, reduced corneal epithelial damage, and lowered levels of proinflammatory cytokines. These results suggest that PLBs-NVs are a safe, natural, and effective therapeutic strategy for DED, supporting their potential for future clinical translation in ocular surface disorders.

Keywords: Corneal epithelial cells, Dry eye disease, Inflammation, Nanovesicles, Protocorm-like bodies of Dendrobium officinale

1. Introduction

Dry eye disease (DED) is a prevalent, multifactorial disorder characterized by tear film instability, ocular surface inflammation, and epithelial damage, often leading to discomfort and visual disturbance [1]. Tear deficiency caused by reduced secretion or excessive evaporation, as well as abnormalities in tear composition or flow, disrupts tear film homeostasis and initiates a cycle of ocular surface stress and inflammation [2,3]. Current treatments primarily focus on symptomatic relief, with limited efficacy in addressing the underlying pathophysiology [4−6].

Natural products have attracted increasing attention in DED management due to their multitarget pharmacological activities and safety profiles. Dendrobium officinale, a valuable traditional Chinese medicinal herb, has been shown to improve lacrimal gland function and promote tear secretion by upregulating aquaporin 5 (AQP5) expression [7]. However, oral or systemic administration of D. officinale extracts often results in low bioavailability at ocular surface sites due to limited local accumulation [8]. Topical delivery offers a more direct approach to treating ocular surface diseases [9]. In recent years, plant-derived nanovesicles (PDNVs) have emerged as promising carriers for drug

* Corresponding author at: Department of Stem Cell Center of Precision Medicine Innovation Institute, He University, No.66 Sishui Street, Hunnan District, Shenyang, 110163, China.
** Corresponding author at: Department of Stem Cell Center of Precision Medicine Innovation Institute, He University, No.66 Sishui Street, Hunnan District, Shenyang, 110163, China.
E-mail addresses: zhangmingqi111@163.com (Z. Mingqi), hsyk2017@163.com (H. Wei).
[1] Co-correspondence for this work.

delivery. First identified in the 1960s, PDNVs are nanoscale vesicles naturally secreted by plants and share functional similarities with mammalian extracellular vesicles [10]. Compared to mammalian vesicles, PDNVs offer several advantages including excellent biocompatibility, low immunogenicity, high structural stability, and efficient cellular uptake [11–17]. These properties enable PDNVs to deliver bioactive compounds such as proteins, lipids, and small RNAs directly to target tissues, offering new opportunities for localized, sustained, and safe therapies.

In this study, we utilized *in vitro*-cultured protocorm-like bodies (PLBs) of D. officinale, which are produced via tissue culture and represent the early developmental form of the pseudobulb. PLBs are recognized as sustainable and standardized alternatives to soil-grown D. officinale, and have been reported to contain similar or even higher levels of pharmacologically active compounds such as polysaccharides, flavonoids, and alkaloids [18–20].

To explore a novel therapeutic strategy for DED, we isolated and characterized nanovesicles from D. officinale PLBs (PLBs-NVs), and evaluated their efficacy in promoting corneal epithelial repair, tear secretion, and inflammation suppression in both *in vitro* and *in vivo* models of DED. Our results suggest that PLBs-NVs are a promising biocompatible and plant-based nanotherapeutic candidate for dry eye treatment.

2. Materials and methods

2.1. Extraction and characterization of nanovesicles derived from in vitro-cultured protocorm-like bodies (PLBs) of Dendrobium officinale (PLBs-NVs)

In vitro-cultured protocorm-like bodies (PLBs) of Dendrobium officinale were provided by Shenyang Kekang Biotechnology Co., Ltd (Shenyang, Liaoning, China). Nanovesicles were extracted following a modified protocol based on Tu et al. [21]. Briefly, 300 g of fresh PLBs were washed three times with Dulbecco's phosphate-buffered saline (DPBS) and air-dried. The PLBs were homogenized at 300 rpm for 10 min to obtain the plant juice. The homogenate was subjected to differential centrifugation to remove debris and collect vesicles. First, low-speed centrifugation was performed at $1000 \times g$ for 10 min, followed by $3000 \times g$ for 10 min to remove fibers and large particles. The resulting supernatant was centrifuged at $10,000 \times g$ for 30 min to eliminate residual impurities. The final supernatant was subjected to ultracentrifugation at $100,000 \times g$ for 60 min (repeated twice) using a Hitachi CP80NX ultracentrifuge (Japan) to pellet the nanovesicles (NVs). The NV pellet was gently resuspended in 500 μL of sterile phosphate-buffered saline (PBS, pH 7.4) and stored at −80 °C until further use.

Prior to use, thawed samples were gently agitated to ensure uniform dispersion. Particle size and concentration, as assessed by NTA and TEM, remained consistent after incubation in PBS or DMEM/F12 (with 1% exosome-depleted FBS) for 48 h at 4 °C and 25 °C, indicating robust colloidal stability. These findings align with prior reports that Leng et al. demonstrated stability in Aloe-derived nanovesicles, and Brucea javanica derived exosome-like nanovesicles showed no significant effect under physiological temperatures in PBS [22,23].

2.1.1. Nanoparticle tracking analysis

Nanoparticle tracking analysis (NTA) was performed using a ZetaView Particle Metrix (Particle Metrix, PMX-120, Germany) to measure the size and concentration of the EVs. The instrument was calibrated with 100 nm polystyrene beads (Thermo Fisher Scientific, Fremont, CA) before use. NTA software was employed to measure the concentration of nanoparticles (particles/mL), with batch processing used for the analysis of each sample.

2.1.2. Negative-stain transmission electron microscopy (TEM)

Transmission electron microscopy (TEM) was utilized to identify nanovesicles. First, 10 μL of the sample extracted by differential centrifugation was placed on a copper grid and allowed to sit for 5–10 min. Excess liquid was removed using filter paper, and the sample was air-dried. The sample was then stained with 10 μL of 2% uranyl acetate. After staining, the sample was visualized using an HT7700 transmission electron microscope (Hitachi, Japan) to confirm the morphology and structure of the nanovesicles.

2.2. Uptake of PLBs-NVs by human corneal epithelial cells

PLBs-derived nanovesicles (PLBs-NVs) were labeled with 10 μM PKH67 green fluorescent dye using the PKH67 Green Fluorescent Cell Linker Mini Kit (Sigma-Aldrich, USA), following the manufacturer's instructions. Briefly, PLBs-NVs were incubated with PKH67 dye for 30 min at 37 °C in the dark. The mixture was then filtered through a 0.22 μm filter and ultracentrifuged at $100,000 \times g$ for 2 h at 4 °C to remove excess unbound dye. The pellet containing fluorescently labeled PLBs-NVs was resuspended in PBS for use in uptake assays.

For the PKH67-alone control group, dye was incubated with PBS (without PLBs-NVs) under identical conditions, followed by ultracentrifugation and resuspension. This control was used to rule out non-specific fluorescence caused by free dye or dye aggregates.

Human corneal epithelial cells (HCECs) were purchased from Guangzhou Jennio Biotech Co., Ltd. (Guangzhou, China). According to the supplier's technical documentation, these are immortalized human corneal epithelial cells, originally isolated from the limbal region of normal human donor eyes, an area enriched in epithelial progenitor cells. The cells were immortalized by SV40 large T antigen transformation and validated for their epithelial phenotype and proliferation capability.

HCECs were seeded on sterile glass coverslips and cultured until they reached appropriate confluence. The culture medium was then replaced with fresh medium containing either PKH67-labeled PLBs-NVs or the PKH67-alone control. After 5 h of incubation at 37 °C in the dark, cells were washed three times with PBS and fixed in 4% paraformaldehyde (PFA; Beyotime Biotechnology, China) for 30 min. After fixation, cells were washed again and observed using a fluorescence inverted microscope (IX51, Olympus, Japan) to evaluate cellular uptake of nanovesicles.

2.3. Cell viability assay

To evaluate the effect of PLBs-NVs on the viability of human corneal epithelial cells, HCECs were seeded in 96-well plates and treated with a range of final concentrations of PLBs-NVs: 0.6×10^9, 1.2×10^9, 1.8×10^9, 2.4×10^9, and 3.0×10^9 particles/mL. Specifically, 10 μL of PLBs-NV stock solutions, prepared at concentrations of 1.2×10^7, 2.4×10^7, 3.6×10^7, 4.8×10^7, and 6.0×10^7 particles/μL, were added to 200 μL of culture medium per well, resulting in the corresponding final particle concentrations.

Cells were cultured in DMEM/F12 medium (Gibco, USA) supplemented with 1% exosome-depleted fetal bovine serum (Gibco, USA) to minimize interference from serum-derived extracellular vesicles while providing the essential nutrients to support cell viability. Control cells were cultured under the same conditions without the addition of PLBs-NVs.

After 24 and 48 h of treatment, cell viability was assessed using the Cell Counting Kit-8 (CCK-8, Beyotime Biotechnology, China) following the instruction manual. The optimal effective concentration of PLBs-NVs was determined based on the ability of PLBs-NVs to maintain cell viability.

2.4. Hypertonic stress model and protective effect of PLBs-NVs

Hyperosmolarity is a widely accepted *in vitro* model used to simulate ocular surface stress conditions associated with dry eye disease (DED). Exposure of human corneal epithelial cells (HCECs) to NaCl-induced hypertonic culture medium mimics tear film hyperosmolarity, leading to inflammation, epithelial damage, and impaired wound healing [24—26].

A 1 M NaCl stock solution was prepared by dissolving analytical-grade sodium chloride (Sinopharm Chemical Reagent Co., Ltd., Cat. No. 10019318, China) in sterile deionized water, filtered through a 0.22 μm membrane, and stored at 4 °C. This stock was diluted into DMEM/F12 medium to achieve final concentrations. The half-maximal lethal concentration (LC50) of NaCl was determined based on HCEC viability after 24 h of exposure. Based on these results, a final concentration of 130 mM NaCl was selected to induce hyperosmotic stress in subsequent experiments.

To evaluate the protective effects of PLBs-derived nanovesicles (PLBs-NVs), HCECs were exposed to two experimental conditions:

- Pre-treatment model: Cells were pre-treated with PLBs-NVs at various final concentrations (0.6×10^9, 1.2×10^9, 1.8×10^9, 2.4×10^9, and 3.0×10^9 particles/mL) for 24 h. Following this, the cells were exposed to 130 mM NaCl for 24 h to assess protective effects.
- Post-treatment model: Cells were first subjected to 130 mM NaCl for 24 h to induce damage. Afterward, cells were washed with sterile PBS (Gibco, USA) and then treated with the same graded concentrations of PLBs-NVs for another 24 h.

Cell viability and proliferation were measured using the CCK-8 assay to evaluate the cytoprotective effect of PLBs-NVs under hyperosmotic conditions. Additional assays assessed wound healing capacity and inflammatory cytokine secretion.

2.5. Scratch wound assay for evaluating the protective effects of PLBs-NVs

To assess the protective effects of PLBs-NVs on wound healing, a scratch assay was performed using human corneal epithelial cells (HCECs) under

both normal and hyperosmotic conditions. Hyperosmotic stress was induced using 130 mM NaCl, as established in previous experiments.

For the hyperosmotic model, HCECs were pretreated with PLBs-NVs for 24 h, followed by scratch induction and continuous exposure to 130 mM NaCl throughout the assay period. Based on prior cell viability and hyperosmotic stress studies, the optimal final concentration of PLBs-NVs was determined to be 1.8×10^9 particles/mL, and this dose was used in all treatment groups.

In the control group, cells were cultured in DMEM/F12 medium supplemented with 1% exosome-depleted FBS, without PLBs-NVs. In the treatment group, the same medium was supplemented with 1.8×10^9 particles/mL PLBs-NVs.

Wound closure was monitored at 12-, 24-, 36-, and 48-h post-scratch using a phase-contrast microscope (Olympus IX51). Wound areas were quantified and compared between treated and untreated groups using ImageJ software.

In addition, culture supernatants were collected from three groups: Normal control, 130 mM NaCl-exposed (hypertonic stress model), and 130 mM NaCl-exposed with PLBs-NVs pre-treatment. These supernatants were used to evaluate the secretion of inflammatory cytokines (IL-1β, IL-6, TNF-α) via ELISA assay following the manufacturer's protocol.

2.6. Murine dry eye model preparation and treatment

A dry eye disease (DED) mouse model was established using a combination of subcutaneous scopolamine injections and exposure to a desiccating environment, following previously described protocols [27,28]. Healthy 6–7-week-old female C57BL/6 mice were obtained from Liaoning Changsheng Biotechnology Co., Ltd. (Shenyang, China) and maintained under specific pathogen-free (SPF) conditions at the Laboratory Animal Center of He University. All animal procedures were approved by the Animal Ethics Committee of He University (Ethics Approval No. 2024051101) and conducted in accordance with international guidelines for animal care and use.

Female mice were selected based on prior studies showing their greater sensitivity to scopolamine-induced lacrimal gland dysfunction and desiccation-related ocular surface damage. Moreover, dry eye is more prevalent and severe in females in both clinical and preclinical research, supporting the translational relevance of this choice [29].

To induce DED, 0.3 mL of 0.25 mg/mL scopolamine solution (Sigma-Aldrich, USA) was injected subcutaneously behind the ear twice daily for 14 days. During this period, mice were housed in a controlled environment with relative humidity $\leq 30\%$ and exposed to continuous airflow using a fan.

PLBs-derived nanovesicles (PLBs-NVs) were administered concurrently with scopolamine injections throughout the induction phase. Mice were randomly assigned into four groups (n = 4 per group): Normal group; DED model group (scopolamine only); PBS treatment group; PLBs-NVs treatment group.

PLBs-NVs were extracted and resuspended in 500 μL of sterile PBS, and particle concentration was quantified using nanoparticle tracking analysis (NTA). Based on in vitro studies, the optimal treatment concentration was 3.6×10^7 particles/μL. The stock solution (original concentration: 2.3×10^8 particles/μL) was diluted accordingly to achieve this target concentration. All dosing solutions were freshly prepared prior to use and verified for particle count by NTA to ensure consistency and reproducibility.

Mice in the treatment group received 5 μL of PLBs-NVs eye drops per eye, three times daily for 14 days. Each microliter of the eye drop formulation contained 3.6×10^7 particles, delivering a total dose of 1.8×10^8 particles per eye per administration.

2.6.1. Corneal fluorescein staining

Corneal epithelial defects were assessed using fluorescein sodium staining, following a standardized scoring system previously described in the literature [30]. Briefly, 1% fluorescein sodium solution (Jingming, G502, China) was applied to the inferior lateral conjunctival sac of the right eye in each mouse. After gentle blinking, the cornea was examined using a slit lamp microscope (Kanghua, HG-914, China) under cobalt blue light on days 7 and 14 post-treatment. The corneal surface was divided into four quadrants, and each quadrant was scored on a scale of 0–4 according to the extent and density of punctate staining: 0: No staining, 1: Slight punctate staining with fewer than 20 dots, 2: Moderate punctate staining with more than 20 dots, but not diffuse, 3: Severe diffuse punctate staining without plaque formation, 4: Positive fluorescein plaque staining. The scores from the four quadrants were summed to yield a total corneal fluorescein staining score (maximum score = 16). Four mice were evaluated per group, and the average score was calculated for analysis.

2.6.2. Tear secretion detection and measurement of inflammatory factors

Tear secretion in mice was assessed using the phenol red thread (PRT) test, a minimally invasive

method widely employed to quantify both basal and reflex tear production. The PRT test is recognized as a reliable and reproducible alternative to the Schirmer test in both clinical and preclinical studies [31]. On days 7 and 14 of treatment, phenol red threads (Jingming, Type I, China) were gently placed in the lateral canthus of each eye for 60 s, after which the length of the wetted red portion was recorded in millimeters as an indicator of tear volume.

Following measurement, each used thread was placed in a sterile 1.5 mL microcentrifuge tube and stored at $-80\ °C$. On the day of analysis, tear proteins were extracted by agitating the thread in 300 µL of sterile $1 \times$ PBS at $4\ °C$ for 2 h. After centrifugation, the supernatant containing tear fluid proteins was collected and used for ELISA quantification of IL-1β, TNF-α, and IL-6 levels, following the manufacturer's protocol (Wuhan Huawei Biotech, China) [32]. Optical density was measured at 450 nm using a microplate reader.

2.6.3. Periodic Acid-Schiff (PAS) staining of conjunctival goblet cells

Conjunctival goblet cell density was evaluated using Periodic Acid-Schiff (PAS) staining, a widely adopted histological method for visualizing mucin-secreting cells in ocular surface tissues [33]. Mouse eyeballs were enucleated post-treatment, fixed in 4% paraformaldehyde, embedded in paraffin, and sectioned into 8 µm-thick slices. The sections were deparaffinized, rehydrated, and then incubated in 0.5% periodic acid oxidation solution (Solarbio, G1281, China) for 8 min at room temperature.

After rinsing with distilled water, the sections were stained with Schiff's reagent in the dark for 20 min, followed by washing under running water for 10 min. Counterstaining was performed with hematoxylin for 1 min. The sections were then sequentially differentiated with dilute hydrochloric acid, blued in ammonia water, washed thoroughly, dehydrated, and mounted.

For quantitative analysis, three central corneal sections were selected per mouse. PAS-positive goblet cells in the conjunctival epithelium were manually counted under a light microscope (Nikon ECLIPSE Ni) and averaged per field to assess goblet cell density.

2.7. Statistical analysis

Data are presented as mean ± standard deviation (SD). All experiments were conducted with a minimum of three independent replicates for cellular assays and included four mice per group in animal studies. Statistical analysis was performed using GraphPad Prism 9.0 (GraphPad Software, San Diego, California, USA). For comparisons between two groups, Student's t-test was utilized, assuming normal or approximately normal distribution of the data. Comparisons among multiple groups were conducted using one-way ANOVA, followed by post hoc Bonferroni test where appropriate. Statistical significance was defined as $p < 0.05$.

3. Results

3.1. Characterization of PLBs-derived nanovesicles (PLBs-NVs)

Nanovesicles were successfully isolated from *in vitro*-cultured Dendrobium officinale protocorm-like bodies (PLBs) using a standard ultracentrifugation protocol (Fig. 1A). Nanoparticle tracking analysis (NTA) revealed that the final suspension contained approximately 2.3×10^{11} particles/mL, with a mean particle diameter of 153.4 nm, indicating a relatively uniform size distribution (Fig. 1B).

Transmission electron microscopy (TEM) further confirmed the vesicular morphology of the purified nanostructures (Fig. 1C). The vesicles appeared round or cup-shaped with electron-dense membranes, and high-magnification images (Fig. 1D) revealed a double-layered membrane structure, consistent with previously reported morphological characteristics of plant-derived extracellular vesicles (PDNVs) [34]. These results collectively support the successful isolation of stable PLBs-NVs with typical extracellular vesicle features.

3.2. Effects of PLBs-NVs on hyperosmolarity-induced stress in human corneal epithelial cells

To investigate cellular uptake, human corneal epithelial cells (HCECs) were incubated with PKH67-labeled PLBs-NVs and observed using fluorescence microscopy. After 5 h of co-culture, fluorescent signals were predominantly localized in the cytoplasm, confirming efficient internalization of PLBs-NVs by HCECs (Fig. 2A).

Next, we evaluated the cytotoxicity of various concentrations of PLBs-NVs. Cell viability was assessed at 24- and 48-h post-treatment using the CCK-8 assay. PLBs-NVs at concentrations ranging from 1.2×10^7 to 4.8×10^7 particles/µL did not significantly affect cell viability. However, a higher concentration of 6×10^7 particles/µL resulted in reduced cell viability at 48 h, suggesting dose-dependent cytostatic effects at high concentrations (Fig. 2B).
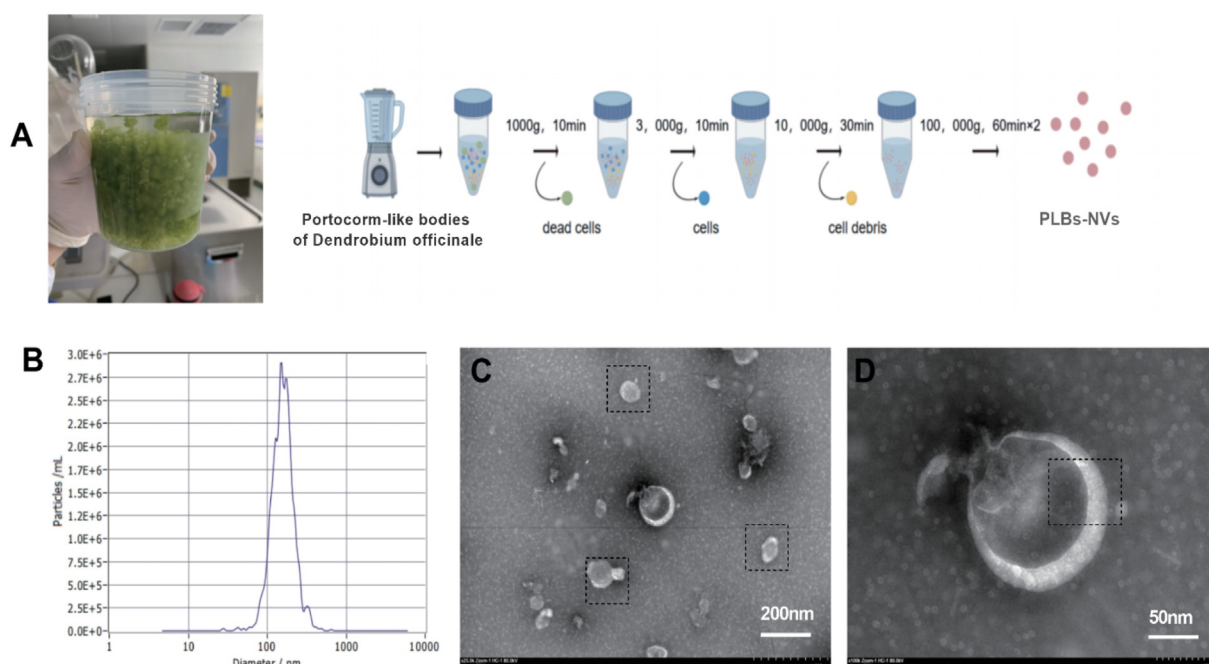
Fig. 1. Characterization of nanovesicles derived from in vitro-cultured protocorm-like bodies (PLBs) of Dendrobium officinale. (A) Representative image of Dendrobium officinale PLBs and schematic diagram of the differential ultracentrifugation protocol used for PLBs-derived nanovesicle (PLBs-NVs) isolation. (B) Nanoparticle tracking analysis (NTA) showing the size distribution and concentration of isolated PLBs-NVs. The average particle size was approximately 153.4 nm. (C) Transmission electron microscopy (TEM) image of PLBs-NVs at 200 nm scale. The vesicles exhibit a typical round-shaped morphology. (D) Enlarged TEM view highlighting the lipid bilayer structure (indicated by dashed black box), confirming the vesicular nature and intact membrane of PLBs-NVs.

To mimic the hyperosmolar environment associated with dry eye, HCECs were exposed to NaCl-induced hypertonic stress. The IC_{50} for NaCl was determined to be 122.48 mM (Fig. 2C), and a concentration of 130 mM NaCl was selected for subsequent stress induction experiments.

We then compared the protective effects of PLBs-NVs when administered either before (pre-treatment) or after (post-treatment) hyperosmotic stress. In the pre-treatment model, PLBs-NVs significantly improved cell viability under hypertonic conditions (Fig. 2D), while no significant benefit was observed with post-treatment (Fig. 2E). Among the tested doses, 3.6×10^7 particles/μL exhibited a robust protective effect in the pre-treatment setting, and was thus selected for use in subsequent experiments. Although slight dose-dependent trends were noted, the differences among effective concentrations were not statistically significant.

3.3. Effects of PLBs-NVs on human corneal epithelial cells wound healing and secretion of inflammatory cytokines

Hyperosmotic conditions can lead to cell apoptosis and result in the loss of corneal epithelium integrity, as well as induce the production of inflammatory cytokines in the ocular surface, which is the key feature of DED. Thus, we examined whether PLBs-NVs could promote the HCECs migration and proliferation. The results demonstrated that PLBs-NVs significantly promoted wound healing in normal condition and hypertonic stress condition by scratch assay. Under normal conditions, treatment with 3.6×10^7 particles/μL PLBs-NVs accelerated wound closure compared to normal group after 36 h treatment (Fig. 3A and B, PLBs-NVs vs. Normal: 0.4103 vs. 0.8362, $p < 0.001$). Similarly, under 130 mM NaCl-induced hyperosmotic stress, treatment with 3.6×10^7 particles/μL PLBs-NVs improved wound healing, with cells showing enhanced closure compared to NaCl model group (PLBs-NVs vs. NaCl: 0.758 vs. 1.071, $p < 0.01$, at 36 h and PLBs-NVs vs. NaCl: 0.544 vs. 0.828, $p < 0.01$, at 48 h). These findings highlight the potential of PLBs-NVs to promote corneal epithelial repair and provide protection under stressful conditions.

To further investigate the anti-inflammatory effect of PLBs-NVs, we measured cytokine levels in the culture supernatants after 48 h of treatment. ELISA results showed that IL-6, IL-1β, and TNF-α were significantly upregulated in the NaCl model group, whereas PLBs-NVs pre-treatment markedly
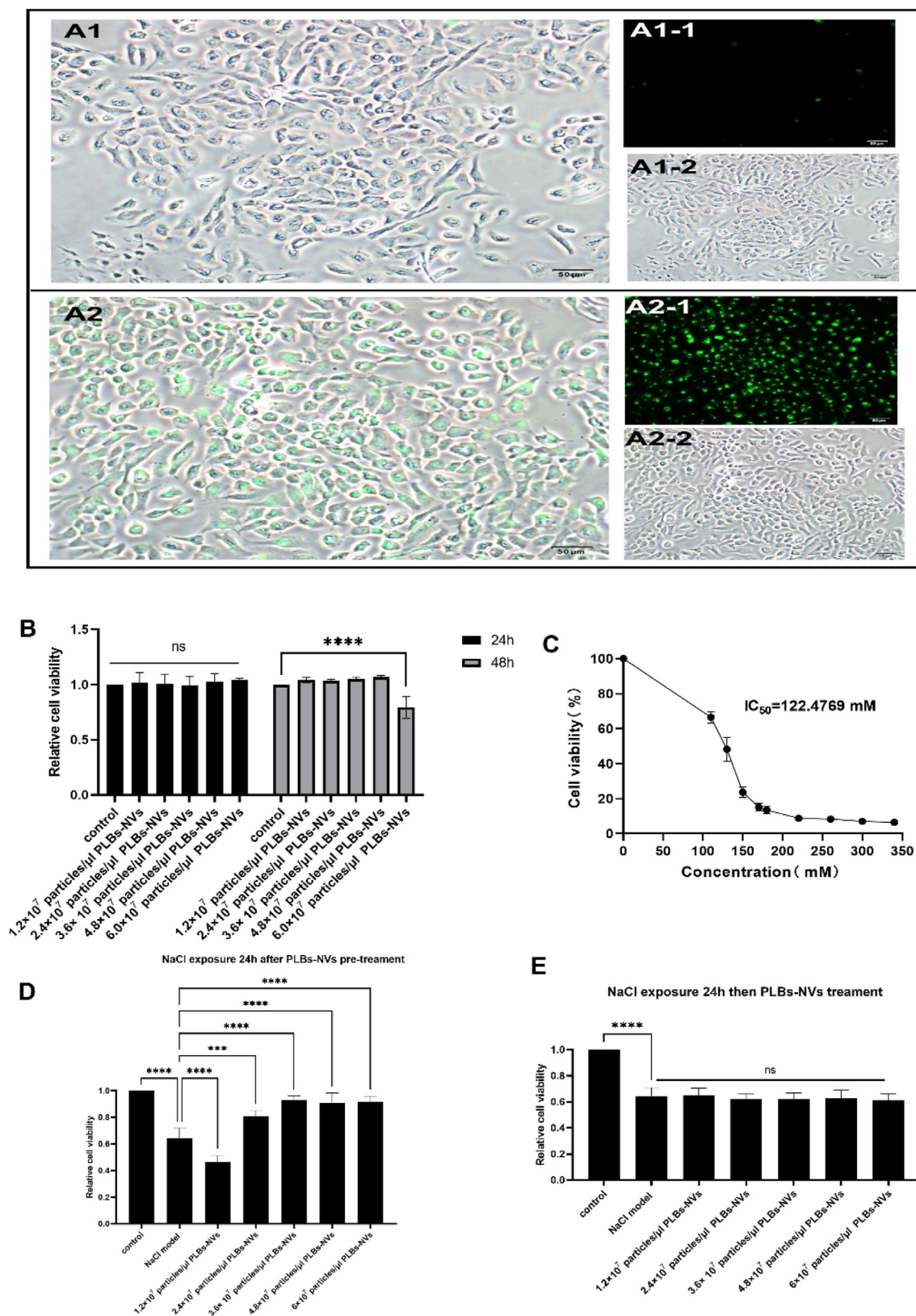
Fig. 2. *PLBs-NVs preserve corneal epithelial cells viability under hypertonic stress in vitro.* (A1) Negative control showing PKH67-alone (without PLBs-NVs) incubation in HCECs, confirming no non-specific dye uptake. (A1-1) Fluorescence image showing uptake of PKH67-alone by HCECs after 5 h incubation. (A1-2) Corresponding bright image. (A2) Representative fluorescent image of human corneal epithelial cells (HCECs) after 5-h incubation with PKH67-labeled PLBs-NVs. Green fluorescence indicates intracellular uptake of vesicles; scale bar: 50 μm. (A2-1) Fluorescence image showing uptake of PKH67–labeled PLBs-NVs by HCECs after 5 h incubation. (A2-2) Corresponding bright image. (B) Cell viability of HCECs following treatment with increasing concentrations of PLBs-NVs (ranging from 0.6×10^9 to 3.0×10^9 particles/mL) for 24 h and 48 h, assessed by CCK-8 assay. (C) Dose-response curve and IC_{50} determination for NaCl-induced hyperosmotic stress in HCECs. (D) Protective effect of HCECs pretreated with PLBs-NVs followed by exposure to 130 mM NaCl. (E) Effect of HCECs exposed to 130 mM NaCl and subsequently treated with PLBs-NVs. ***$p < 0.001$, ****$p < 0.0001$, ns = not significant, compared to the NaCl-only group.
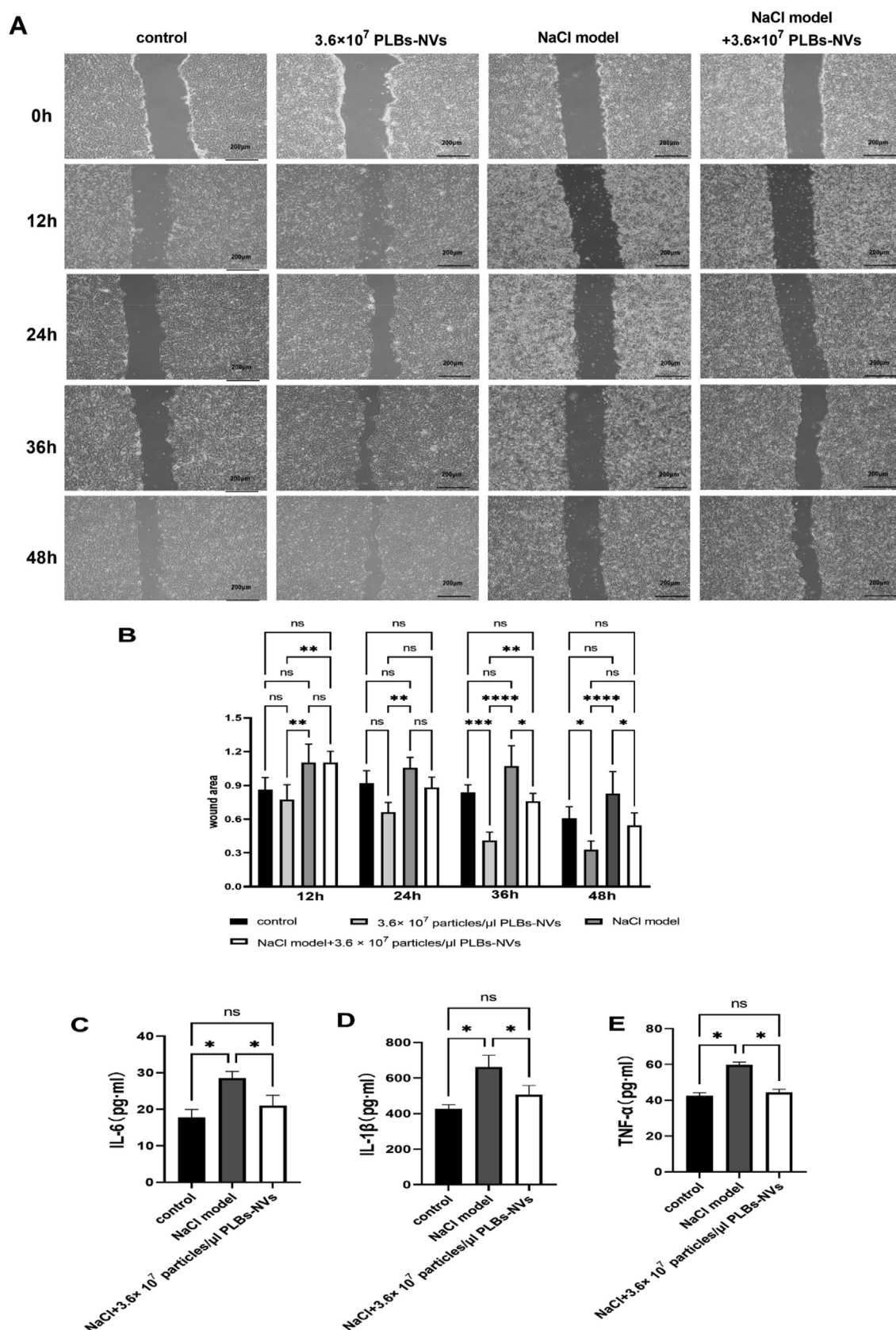
Fig. 3. *PLBs-NVs promote wound healing of human corneal epithelial cells and suppress inflammatory cytokine secretion. (A) Representative microscopic images of scratch wound closure in human corneal epithelial cells (HCECs) under normal and hypertonic conditions (130 mM NaCl), with or without PLBs-NVs treatment (1.8 × 10⁹ particles/mL), captured at 0, 12-, 24-, 36-, and 48-h post-scratch. Scale bar = 200 μm. (B) Quantitative analysis of wound area at different time points, showing accelerated wound closure in PLBs-NVs-treated groups. (C—E) ELISA analysis of proinflammatory cytokines IL-6 (C), IL-1β (D), and TNF-α (E) levels in the culture supernatant at 48 h under hypertonic stress conditions, demonstrating significant suppression by PLBs-NVs. ****p < 0.0001, ***p < 0.001, **p < 0.01, *p < 0.05, ns = not significant (vs. NaCl-only control).*

inhibited their expression, indicating potent anti-inflammatory activity under hyperosmotic conditions (Fig. 3C–E).

3.4. Topical treatment of PLBs-NVs alleviate ocular surface damage and inflammation in a mouse dry eye model

To evaluate the therapeutic potential of PLBs-NVs for dry eye disease, we utilized a mouse model induced by scopolamine combined with a desiccated environment. The process of establishing the model and subsequent treatments with PLBs-NVs is illustrated in Fig. 4A. Treatment effects were assessed using fluorescein sodium staining, tear volume measurement, and inflammatory cytokine quantification. As shown in Fig. 4B, fewer green-stained puncta were observed in corneas of mice treated with PLBs-NVs, while the DED model and PBS groups exhibited widespread staining, indicating significant corneal epithelial damage. Quantitative analysis confirmed that fluorescein scores were significantly lower in the PLBs-NVs group on both day 7 and day 14 compared to the model and PBS groups (Fig. 4C; Day 7: PLBs-NVs vs. Model, 1.75 vs. 4.75, $p < 0.05$; Day 14: PLBs-NVs vs. Model, 0.85 vs. 6.25, $p < 0.0001$; PLBs-NVs vs. PBS, 0.85 vs. 4.0, $p < 0.05$).

The phenol red cotton thread test was performed to evaluate the effect of PLBs-NVs on tear production. Then we collected tear fluid and their inflammatory factors were measured using ELISA assay. On the 7th day, the tear volume in model and Pbs groups were significantly lower than that of control group, while the PLBs-NVs treatment group exhibited a slight increase tear production compared with the DED model group and Pbs group. On the 14th day, PLBs-NVs group showed significantly increase of tear secretion, while the DED model and Pbs groups still maintained a low level of tear volume (Fig. 4D). Tear samples were further analyzed for cytokine expression. The DED model and PBS groups exhibited elevated IL-6, IL-1β, and TNF-α levels as the treatment time extended, while the PLBs-NVs group showed a pronounced reduction in these inflammatory mediators, confirming the anti-inflammatory efficacy of topical NV application (Fig. 4E–G).

3.5. PLBs-NVs prevent the loss of Goblet Cells and improve corneal structure

To assess histological changes, Periodic Acid-Schiff (PAS) staining was performed to evaluate conjunctival goblet cell density. On day 14, the PLBs-NVs group maintained a significantly higher number of PAS-positive goblet cells compared to both the DED model and PBS groups (Fig. 5A and B; PLBs-NVs vs. Model: 42.44 vs. 13.64, $p < 0.05$; PLBs-NVs vs. PBS: 42.44 vs. 15.77, $p < 0.01$).

Histological examination of the cornea revealed that corneal thickness was reduced in the PLBs-NVs-treated mice, suggesting alleviation of corneal edema, likely due to reduced inflammation. Additionally, the epithelial layer exhibited a compact and continuous morphology in the PLBs-NVs group, in contrast to the disrupted architecture observed in untreated controls (Fig. 5A and C).

4. Discussion

Dry eye disease (DED) is a chronic, multifactorial ocular surface disorder characterized by tear film instability, hyperosmolarity, ocular surface inflammation, and epithelial cell damage. Its pathogenesis is best described by the "vicious cycle" theory, where tear film disruption and increased osmolarity lead to epithelial stress and apoptosis, triggering the release of inflammatory cytokines (e.g., IL-1β, IL-6, TNF-α), which in turn perpetuate tear film instability and surface damage [24]. Therefore, effective treatment should not only suppress inflammation but also restore epithelial integrity and stimulate tear production to break this cycle.

In this study, we demonstrated that nanovesicles derived from in vitro-cultured protocorm-like bodies (PLBs) of Dendrobium officinale (PLBs-NVs) possess therapeutic effects that act on multiple key mechanisms in the DED pathological cascade. In vitro, PLBs-NVs preserved human corneal epithelial cell (HCEC) viability under hyperosmotic conditions, promoted wound closure in scratch assays, and significantly suppressed NaCl-induced proinflammatory cytokine release (IL-6, IL-1β, TNF-α). These findings indicate that PLBs-NVs can protect epithelial cells from osmotic stress and accelerate their repair—crucial steps for maintaining the integrity of the ocular surface barrier and breaking the vicious cycle of DED [35]. In vivo, topical administration of PLBs-NVs in a desiccating stress-induced mouse model of DED improved tear secretion, reduced corneal fluorescein staining, preserved conjunctival goblet cells, and significantly decreased the expression of inflammatory cytokines in tears. These therapeutic effects align directly with the three primary pathophysiological targets in DED: (1) restoring epithelial barrier function, (2) reducing ocular surface inflammation, and (3) stabilizing the tear film.
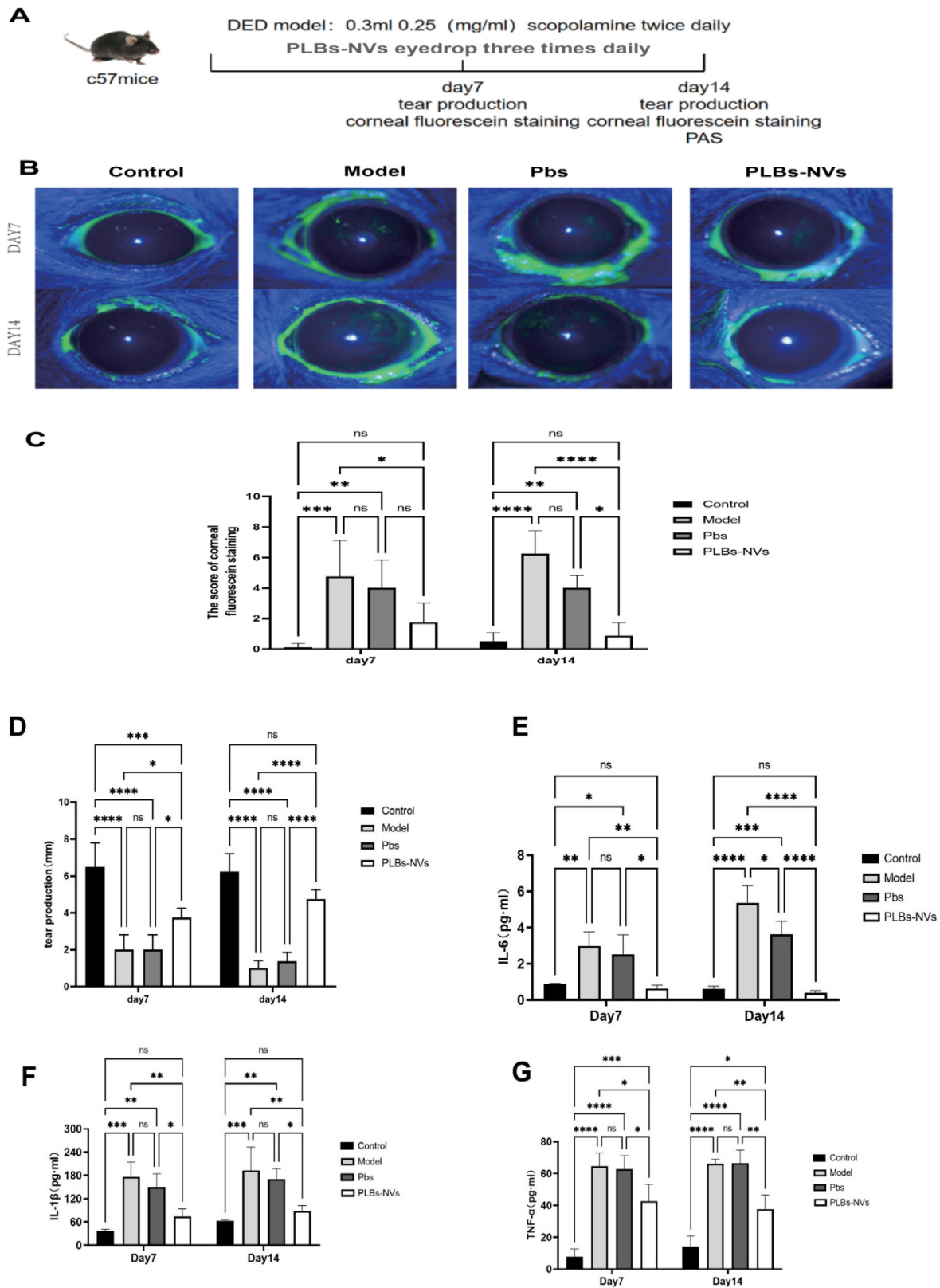
Fig. 4. *PLBs-NVs alleviate ocular surface damage and reduce proinflammatory cytokine levels in a murine dry eye model.* (A) Schematic diagram illustrating the establishment of the dry eye disease (DED) model via scopolamine injection combined with desiccating stress, and the treatment timeline for topical PLBs-NVs application. (B) Representative fluorescein sodium-stained corneal images from each group at day 7 and day 14. Green dots indicate punctate epithelial defects. (C) Corneal fluorescein staining scores quantified across four quadrants based on density and severity of epithelial defects. (D) Phenol red thread test showing tear secretion levels in each group at days 7 and 14. (E–G) ELISA quantification of inflammatory cytokines IL-6 (E), IL-1β (F), and TNF-α (G) in mouse tear fluid. PLBs-NVs significantly reduced cytokine expression compared to DED and PBS groups. ****$p < 0.0001$, ***$p < 0.001$, **$p < 0.01$, *$p < 0.05$, ns = not significant (vs. model or PBS control groups as indicated).
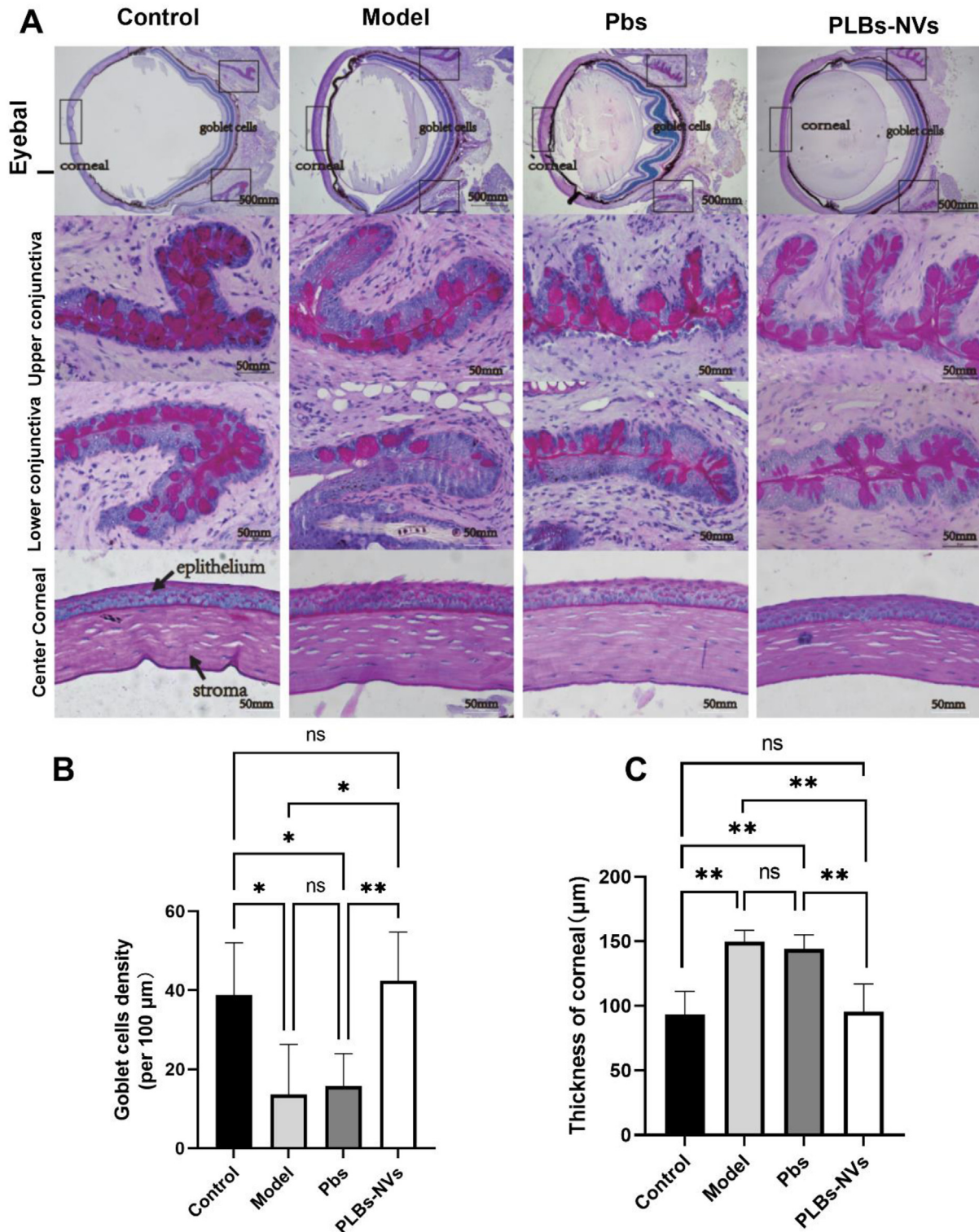
Fig. 5. *PLBs-NVs reduce goblet cell loss and preserve corneal structure in DED mice.* (A) Representative PAS-stained images showing histological morphology of the eyeball and ocular surface tissues after 14 days of treatment. Upper row: whole eyeball sections. Middle row: upper and lower conjunctival regions, highlighting PAS-positive goblet cells (dark red-purple). Lower row: corneal cross-sections displaying epithelial and stromal architecture. (B) Quantification of goblet cell density in conjunctival sections. Goblet cells were manually counted in three representative regions per eye. (C) Measurement of central corneal thickness from stained sections using ImageJ. PLBs-NVs significantly reduced corneal edema and preserved normal tissue structure. *p < 0.01, p < 0.05, ns = not significant.

Although polysaccharides and flavonoids are traditionally recognized as the key active components of Dendrobium officinale with known antioxidant and immunomodulatory effects [36,37], the emergence of plant-derived nanovesicles (PDNVs) introduces a new paradigm in natural product-based therapy. The mechanistic basis for these protective effects may lie in the natural cargo of PDNVs, which are known to carry small RNAs, proteins, lipids, and antioxidants. Previous studies have suggested that PDNVs can facilitate interspecies communication and modulate mammalian cell function without eliciting immune rejection. Compared to conventional pharmacological carriers, PDNVs offer higher biocompatibility, intrinsic bioactivity, and ease of large-scale production [38].

Compared to current treatments for DED—including artificial tears, corticosteroids, cyclosporine A, and lifitegrast—which mainly provide symptomatic relief or target inflammation, PLBs-NVs offer a multifunctional therapeutic strategy. Their ability to simultaneously promote epithelial repair, suppress inflammatory mediators, and restore tear secretion positions them as a promising candidate for disease-modifying therapy rather than temporary palliation [39].

Importantly, our study utilized *in vitro*-cultured PLBs as a sustainable and standardized source of nanovesicles, offering batch consistency and scalability that overcomes the variability associated with field-grown Dendrobium. This biotechnological approach enhances the feasibility of clinical translation and large-scale application.

In conclusion, PLBs-NVs represent a novel and biocompatible nanotherapeutic derived from a traditional medicinal plant. By targeting key elements of DED pathogenesis—epithelial damage, inflammation, and tear deficiency—they hold promise as an effective, natural treatment for chronic ocular surface disorders. Further mechanistic studies and long-term safety assessments will be essential to advance PLBs-NVs toward clinical application.

5. Conclusion

In summary, our study provides compelling evidence that nanovesicles derived from *in vitro*-cultured protocorm-like bodies (PLBs) of Dendrobium officinale (PLBs-NVs) represent a promising and multifaceted therapeutic strategy for dry eye disease (DED). *In vitro*, PLBs-NVs preserved corneal epithelial cell viability under hyperosmotic stress, promoted wound closure, and suppressed pro-inflammatory cytokine production. *In vivo*, topical application of PLBs-NVs in a desiccating stress-induced DED mouse model effectively restored tear secretion, preserved corneal epithelial integrity, maintained conjunctival goblet cell density, and downregulated key inflammatory mediators such as IL-6, IL-1β, and TNF-α.

These findings collectively demonstrate that PLBs-NVs exert beneficial effects on multiple pathological aspects of DED, including epithelial damage, tear film instability, and chronic inflammation. Given their plant-derived origin, biocompatibility, and ease of topical administration, PLBs-NVs hold substantial potential as a novel therapeutic modality for the clinical management of DED. Further investigations into the molecular mechanisms and long-term safety profiles of PLBs-NVs will support their future translation into clinical application.

Conflicts of interest

The authors report no conflicts of interest in this work.

Acknowledgments

References

[1] Rolando M, Merayo-Lloves J. Management strategies for evaporative dry eye disease and future perspective. Curr Eye Res 2022;47:813—23. https://doi.org/10.1080/02713683.2022.2039205.

[2] Mohamed HB, Abd El-Hamid BN, Fathalla D, Fouad EA. Current trends in pharmaceutical treatment of dry eye disease: a review. Eur J Pharmaceut Sci 2022;175:106206. https://doi.org/10.1016/j.ejps.2022.106206.

[3] Nagai N, Otake H. Novel drug delivery systems for the management of dry eye. Adv Drug Deliv Rev 2022;191:114582. https://doi.org/10.1016/j.addr.2022.114582.

[4] Marshall LL, Hayslett RL. Dry eye disease: focus on prescription therapy. Sr Care Pharm 2023;38:239—51. https://doi.org/10.4140/TCP.n.2023.239.

[5] McCann P, Kruoch Z, Lopez S, Malli S, Qureshi R, Li T. Interventions for dry eye: an overview of systematic reviews. JAMA Ophthalmol 2024;142:58—74. https://doi.org/10.1001/jamaophthalmol.2023.5751.

[6] Messmer EM. The pathophysiology, diagnosis, and treatment of dry eye disease. Dtsch Arztebl Int 2015;112:71—81. https://doi.org/10.3238/arztebl.2015.0071. 82.

[7] Ling J, Chan CL, Ho CY, Gao X, Tsang SM, Leung PC, et al. The extracts of dendrobium alleviate dry eye disease in rat model by regulating aquaporin expression and MAPKs/NF-kappaB Signalling. Int J Mol Sci 2022;23. https://doi.org/10.3390/ijms231911195.

[8] Yi Q, Liang P, Liang D, Cao L, Sha S, Jiang X, et al. Improvement of polydopamine-loaded salidroside on osseointegration of titanium implants. Chin Med 2022 Feb 21;17:26. https://doi.org/10.1186/s13020-022-00569-9.

[9] Akhter MH, Ahmad I, Alshahrani MY, Al-Harbi AI, Khalilullah H, Afzal O, et al. Drug delivery challenges and current progress in nanocarrier-based ocular therapeutic system. Gels 2022;8:82. https://doi.org/10.3390/gels8020082.

[10] Jensen WA. The composition and ultrastructure of the Nucellus in Cotton. J Ultrastruct Res 1965;13:112–28. https://doi.org/10.1016/S0022-5320(65)80092-2.

[11] Chu K, Liu J, Zhang X, Wang M, Yu W, Chen Y, et al. Herbal medicine-derived exosome-like nanovesicles: a rising star in cancer therapy. Int J Nanomed 2024;19:7585–603. https://doi.org/10.2147/IJN.S477270.

[12] Liu X, Lou K, Zhang Y, Li C, Wei S, Feng S. Unlocking the medicinal potential of plant-derived extracellular vesicles: current progress and future perspectives. Int J Nanomed 2024;19:4877–92. https://doi.org/10.2147/IJN.S463145.

[13] Logozzi M, Di Raimo R, Mizzoni D, Fais S. The potentiality of plant-derived nanovesicles in human health-a comparison with human exosomes and artificial nanoparticles. Int J Mol Sci 2022;23:4919. https://doi.org/10.3390/ijms23094919.

[14] Sall IM, Flaviu TA. Plant and mammalian-derived extracellular vesicles: a new therapeutic approach for the future. Front Bioeng Biotechnol 2023;11:1215650. https://doi.org/10.3389/fbioe.2023.1215650.

[15] Kim J, Li S, Zhang S, Wang J. Plant-derived exosome-like nanoparticles and their therapeutic activities. Asian J Pharm Sci 2022;17:53–69. https://doi.org/10.1016/j.ajps.2021.05.006.

[16] Leng Y, Yang L, Zhu H, Li D, Pan S, Yuan F. Stability of blueberry extracellular vesicles and their gene regulation effects in intestinal caco-2 cells. Biomolecules 2023;13:1412. https://doi.org/10.3390/biom13091412.

[17] Kim K, Park J, Sohn Y, Oh CE, Park JH, Yuk JM, et al. Stability of plant leaf-derived extracellular vesicles according to preservative and storage temperature. Pharmaceutics 2022;14:457. https://doi.org/10.3390/pharmaceutics14020457.

[18] Chen Q, Zhang C, Chen Y, Wang C, Lai Z. Transcriptomic analysis for diurnal temperature differences reveals gene-regulation-network response to accumulation of bioactive ingredients of protocorm-like bodies in Dendrobium officinale. Plants (Basel) 2024;13:874. https://doi.org/10.3390/plants13060874.

[19] Wei M, Yang CY, Wei SH. Enhancement of the differentiation of protocorm-like bodies of Dendrobium officinale to shoots by ultrasound treatment. J Plant Physiol 2012;169:770–4. https://doi.org/10.1016/j.jplph.2012.01.018.

[20] Wei M, Jiang ST, Luo JP. Enhancement of growth and polysaccharide production in suspension cultures of protocorm-like bodies from Dendrobium huoshanense by the addition of putrescine. Biotechnol Lett 2007;29:495–9. https://doi.org/10.1007/s10529-006-9248-7.

[21] Tu J, Jiang F, Fang J, Xu L, Zeng Z, Zhang X, et al. Anticipation and verification of dendrobium-derived nanovesicles for skin wound healing targets, predicated upon immune infiltration and senescence. Int J Nanomed 2024;19:1629–44. https://doi.org/10.2147/IJN.S438398.

[22] Zeng L, Wang H, Shi W, Chen L, Chen T, Chen G, et al. Aloe derived nanovesicle as a functional carrier for indocyanine green encapsulation and phototherapy. J Nanobiotechnol 2021;19:439. https://doi.org/10.1186/s12951-021-01195-7.

[23] Yan G, Xiao Q, Zhao J, Chen H, Xu Y, Tan M, et al. Brucea javanica derived exosome-like nanovesicles deliver miRNAs for cancer therapy. J Contr Release 2024;367:425–40. https://doi.org/10.1016/j.jconrel.2024.01.060.

[24] Bron AJ, de Paiva CS, Chauhan SK, Bonini S, Gabison EE, Jain S, et al. TFOS DEWS II pathophysiology report. Ocul Surf 2019;17:842. https://doi.org/10.1016/j.jtos.2019.08.007.

[25] Song C, Seong H, Yoo WS, Choi MY, Varga RD, Eom Y, et al. Diquafosol improves corneal wound healing by inducing NGF expression in an experimental dry eye model. Cells 2024;13:1251. https://doi.org/10.3390/cells13151251.

[26] Igarashi T, Fujimoto C, Suzuki H, Ono M, Iijima O, Takahashi H, et al. Short-time exposure of hyperosmolarity triggers interleukin-6 expression in corneal epithelial cells. Cornea 2014;33:1342–7. https://doi.org/10.1097/ICO.0000000000000256.

[27] De Paiva CS, Volpe EA, Gandhi NB, Zhang X, Zheng X, Pitcher JD, et al. Disruption of TGF-β signaling improves ocular surface epithelial disease in experimental autoimmune keratoconjunctivitis sicca. PLoS One 2011;6:e29017. https://doi.org/10.1371/journal.pone.0029017.

[28] Chu C, Huang Y, Ru Y, Lu X, Zeng X, Liu K, et al. alpha-MSH ameliorates corneal surface dysfunction in scopolamine-induced dry eye rats and human corneal epithelial cells via enhancing EGFR expression. Exp Eye Res 2021;210:108685. https://doi.org/10.1016/j.exer.2021.108685.

[29] Maruoka S, Inaba M, Ogata N. Activation of dendritic cells in dry eye mouse model. Investig Ophthalmol Vis Sci 2018;59:3269–77. https://doi.org/10.1167/iovs.17-22550.

[30] Zhang C, Li K, Yang Z, Wang Y, Si H. The effect of the aqueous extract of Bidens Pilosa L. on androgen deficiency dry eye in rats. Cell Physiol Biochem 2016;39:266–77. https://doi.org/10.1159/000445622.

[31] Hao Y, Jin T, Zhu L, Zhao M, Wang S, Li Z, et al. Validation of the phenol red thread test in a Chinese population. BMC Ophthalmol 2023;23:498. https://doi.org/10.1186/s12886-023-03250-3.

[32] Kecskeméti G, Tóth-Molnár E, Janáky T, Szabó Z. An extensive study of phenol red thread as a novel non-invasive tear sampling technique for proteomics studies: comparison with two commonly used methods. Int J Mol Sci 2022;23:8647. https://doi.org/10.3390/ijms23158647.

[33] Astolfi G, Lorenzini L, Gobbo F, Sarli G, Versura P. Comparison of trehalose/hyaluronic acid (HA) vs. 0.001% hydrocortisone/HA eyedrops on signs and inflammatory markers in a desiccating model of dry eye disease (DED). J Clin Med 2022;11:1518. https://doi.org/10.3390/jcm11061518.

[34] Di Gioia S, Hossain MN, Conese M. Biological properties and therapeutic effects of plant-derived nanovesicles. Open Med (Wars) 2020;15:1096–122. https://doi.org/10.1515/med-2020-0160.

[35] Wu W, Zhang B, Wang W, Bu Q, Li Y, Zhang P, et al. Plant-derived exosome-like nanovesicles in chronic wound healing. Int J Nanomed 2024;19:11293–303. https://doi.org/10.2147/IJN.S485441.

[36] Chen YF, Zhang DD, Hu DB, Li XN, Luo JF, Duan XY, et al. Alkaloids and flavonoids exert protective effects against UVB-induced damage in a 3D skin model using human keratinocytes. Results Chem 2022;4:2211–7156. https://doi.org/10.1016/j.rechem.2022.100298. 100298, ISSN.

[37] Ye HY, Shang ZZ, Zhang FY, Zha XQ, Li QM, Luo JP. Dendrobium huoshanense stem polysaccharide ameliorates alcohol-induced gastric ulcer in rats through Nrf2-mediated strengthening of gastric mucosal barrier. Int J Biol Macromol 2023;236:124001. https://doi.org/10.1016/j.ijbiomac.2023.124001.

[38] Fu W, Zhang P, Wang W, Du M, Ni R, Sun Y. Frontiers of plant-derived exosomes from research methods to pharmaceutical applications in plant-based therapeutics. Curr Drug Deliv 2024 Jun 11. https://doi.org/10.2174/0115672018305953240606063911.

[39] Jones L, Downie LE, Korb D, Benitez-Del-Castillo JM, Dana R, Deng SX, et al. TFOS DEWS II management and therapy report. Ocul Surf 2017;15:575–628. https://doi.org/10.1016/j.jtos.2017.05.006.